

# Rapid Gel Formation and Adhesion in Photocurable and Biodegradable Block Copolymers with High DOPA Content

Bruce P. Lee,<sup>†</sup> Chi-Yang Chao,<sup>‡</sup> F. Nelson Nunalee,<sup>‡</sup> Emre Motan,<sup>†</sup>  
Kenneth R. Shull,<sup>‡</sup> and Phillip B. Messersmith<sup>\*,‡</sup>

Department of Biomedical Engineering, Northwestern University, 2145 N Sheridan Road,  
Evanston, Illinois 60208, and Department of Materials Science and Engineering,  
Northwestern University, 2220 Campus Drive, Evanston, Illinois 60208

Received August 29, 2005; Revised Manuscript Received December 29, 2005

**ABSTRACT:** Marine mussels anchor to a variety of surfaces in turbulent intertidal zones through the use of adhesive plaques formed from hardened mussel adhesive proteins (MAPs). It is believed that 3,4-dihydroxyphenylalanine (DOPA) imparts both water-resistant adhesive characteristics and rapid curing ability to MAPs. In this paper, DOPA-modified triblock copolymers were synthesized and used to form adhesive hydrogels. Amphiphilic block copolymers with DOPA content as high as 10 wt % were prepared, and aqueous solutions of the polymers rapidly (<1 min) formed hydrogels by photopolymerization of methacrylate end groups attached to the hydrophobic segments. Contact mechanics adhesion tests were performed on the photocured hydrogels, and it was shown that incorporating DOPA into the polymer structure significantly enhanced work of adhesion to titanium surfaces submerged in an aqueous medium. Work of adhesion values as high as 410 mJ/m<sup>2</sup> were recorded for polymers containing 10 wt % DOPA, although the introduction of Lys in the form of a DOPA–Lys copolypeptide reduced the work of adhesion. Oxidation of DOPA was shown to reduce work of adhesion to Ti, confirming earlier studies suggesting that the catecholic form of DOPA is largely responsible for adhesion to metal oxide surfaces. The DOPA-containing block copolymers described in this study are candidates for use as adhesive biomaterials for medical applications.

## Introduction

Amphiphilic degradable block copolymers designed for use as rapidly photopolymerizable hydrogels were first reported by Sawhney et al. in 1993.<sup>1</sup> These polymers were designed as ABA triblock copolymers consisting of a poly(ethylene glycol) (PEG) “B” block flanked by hydrolyzable oligomeric poly( $\alpha$ -hydroxy acid) “A” segments and end-capped with polymerizable acrylate esters. These polymers have the attractive characteristics of being easily formulated into aqueous solutions capable of rapid polymerization into hydrogels by light activation and are degradable by virtue of the polyester segments. These photocurable block copolymers have been studied for various biomedical applications, including postsurgical adhesion barriers<sup>2</sup> and matrices for drug<sup>3</sup> and cell<sup>4</sup> encapsulation.

A useful property of these polymers is their ability to be rapidly polymerized from a liquid precursor solution into a hydrogel in as little as 10–20 s under physiologic conditions.<sup>1</sup> Such rapid polymerization is desired in certain clinically used materials such as surgical sealants and adhesives, where sol–gel transformation is used to seal tissue defects or adhere tissue surfaces together, respectively. There are reports of photopolymerizable ABA block copolymers being investigated as surgical sealants;<sup>5,6</sup> however, to our knowledge the adhesive properties of these gels have never been reported. As these polymers are composed primarily of PEG, a nonadhesive polymer, we hypothesize that chemical modification of the polymer may be necessary for enhancing adhesion to tissue and implant surfaces.

Mussel adhesive proteins (MAPs) are specialized adhesive proteins containing high concentrations of lysine and the unusual

amino acid 3,4-dihydroxyphenyl-L-alanine (DOPA).<sup>7</sup> MAPs are an essential component of the attachment mechanism used by the organisms, and the water-resistant adhesive properties of these proteins have inspired several research groups to mimic these proteins in synthetic polymers.<sup>8–18</sup> In our laboratory we recently incorporated DOPA into polymer hydrogels via photopolymerization of N-methacrylated DOPA monomers with PEG-diacrylate.<sup>16</sup> Although DOPA was chemically integrated into the PEG-based hydrogel, the presence of DOPA lengthened the gelation time and reduced the moduli of the photocured gels.<sup>16</sup> These observations were attributed to the phenolic nature of the catechol side chain of DOPA and its ability to act as a radical scavenger.<sup>19–22</sup>

In this paper we describe a series of new DOPA-containing biodegradable block copolymers that rapidly photopolymerize into adhesive hydrogels. A new synthetic strategy is reported that allows the facile coupling of DOPA-containing peptides to the central PEG segment of the triblock copolymers and facilitates control of peptide composition and DOPA concentration in a straightforward manner. Aqueous solutions of the peptide-modified block copolymers were shown to rapidly photopolymerize into hydrogels upon exposure to long wavelength UV radiation, and wet adhesion of the hydrogels to a metal oxide surface was significantly enhanced in hydrogels functionalized with DOPA-containing peptides.

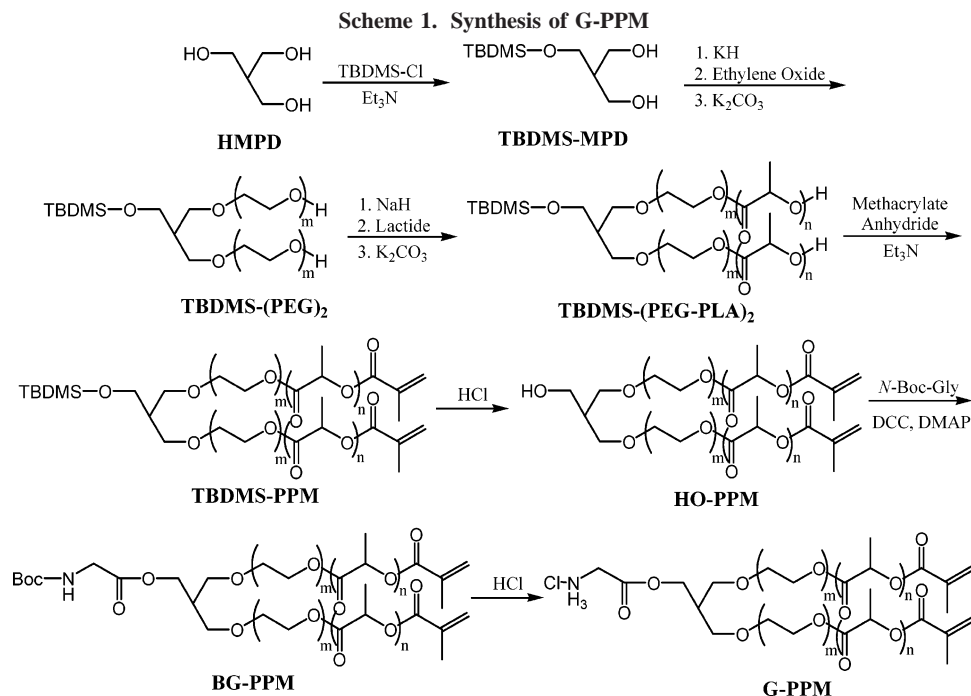
## Experimental Section

**Materials.** 99% anhydrous HCl, 2-hydroxymethylpropane-1,3-diol (HMPD), acetyl anhydride, sodium hydride (60 wt % in mineral oil, NaH), 3,6-dimethyl-1,4-dioxane-2,5-dione (LA), *tert*-butyldimethylsilyl chloride (TBDMS-Cl), redistilled pyridine, methacrylic anhydride, 4-(dimethylamino)pyridine (DMAP), 4 M HCl in dioxane, DOPA, di-*tert*-butyl dicarbonate (Boc<sub>2</sub>O), 2,2'-dimethoxy-2-phenylacetonephenone (DMPA), 1-vinyl-2-pyrrolidone (VP), and

<sup>†</sup> Department of Biomedical Engineering.

<sup>‡</sup> Department of Materials Science and Engineering.

\* To whom correspondence should be addressed: Ph (847) 467-5273; Fax (847) 491-4928; e-mail philm@northwestern.edu.



1 M dibutylmagnesium in heptane were purchased from Aldrich (Milwaukee, WI). Ethylene oxide was from Fisher Chemicals (Fairlawn, NJ), and Contrad 70 was purchased from Decon Labs, Inc. (Bryn Mawr, PA). 20% phosgene in toluene and potassium hydride (35 wt % in mineral oil, KH) was from Fluka (Milwaukee, WI). Hydroxybenzotriazole (HOBt) was obtained from Novabiochem Corp. (La Jolla, CA). *O*-(Benzotriazol-1-yl)-*N,N,N',N'*-tetramethyluronium hexafluorophosphate (HBTU), *N*-Boc-glycine (*N*-Boc-Gly), and *N,N'*-dicyclohexylcarbodiimide (DCC) were acquired from Advanced ChemTech (Louisville, KY). *N*- $\epsilon$ -Fmoc-Lysine was purchased from Bachem Bioscience Inc. (King of Prussia, PA), and silicon (Si) wafer was purchased from University Wafer (Boston, MA). *N*-Carboxyanhydrides (NCAs) of DOPA (diacetyl-DOPA-NCA) and Lysine (Fmoc-Lys-NCA) were prepared by following literature procedures.<sup>23,24</sup>

**Overview of Polymer Synthesis.** The general approach employed to synthesize rapidly photocurable amphiphilic block copolymers functionalized with DOPA peptides is illustrated in Schemes 1 and 2. First, the monoprotected triol TBDMS-MPD was used to initiate stepwise anionic ring-opening polymerization of ethylene oxide followed by lactide to afford the protected PEG-PLA block copolymer TBDMS-(PEG-PLA)<sub>2</sub>. Following methacrylation of the PLA end groups and removal of TBDMS, coupling of *N*-Boc-Gly and deprotection of Boc yielded the glycine-functionalized block copolymer G-PPM (Scheme 1). G-PPM then served as a versatile starting point for synthesis of several block copolymers containing adhesive peptides, formed either by standard peptide coupling chemistry or by polymerization of NCA monomers (Scheme 2). The latter approach builds off of recent reports on the use of polymer-bound primary amines to initiate polymerization of NCA monomers.<sup>25–29</sup>

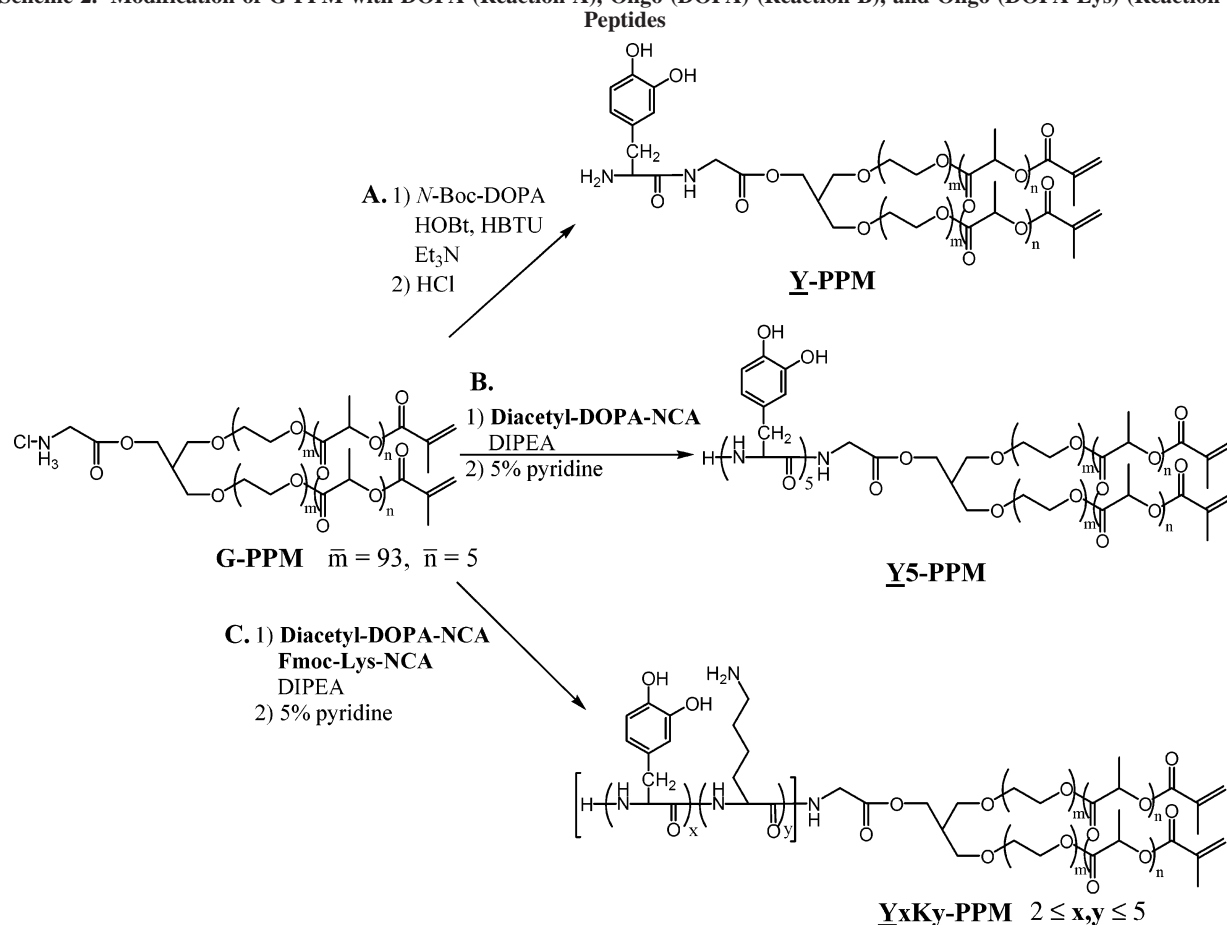
**Synthesis of 2-(*tert*-Butyldimethylsilanyloxymethyl)propane-1,3-diol (TBDMS-MPD).** TBDMS-MPD was synthesized by slight modification of a published procedure.<sup>30</sup> 2 g of HMPD (17.9 mmol) was dissolved in 50 mL of anhydrous acetonitrile at 50 °C, and 2.13 mL of Et<sub>3</sub>N (15.2 mmol) was added to the mixture. 2.28 g of TBDMS-Cl (14.7 mmol) in 20 mL of anhydrous acetonitrile was added dropwise. The reaction mixture was stirred at room temperature for 20 h. 200 mL of ethyl ether was added, and the organic mixture was washed with 5% K<sub>2</sub>CO<sub>3</sub> two times. The organic layer was dried over MgSO<sub>4</sub> and concentrated by rotary evaporation. The crude oil was eluted through a silica gel column in hexane with increasing ethyl acetate concentration (0–100% ethyl acetate in hexane). After evaporating the solvents, 1.5 g of clear, colorless

liquid was obtained. <sup>1</sup>H NMR (500 MHz, CDCl<sub>3</sub>):  $\delta$  3.83 (m, 6 H, O-CH<sub>2</sub>-CH); 2.74 (br s, 2 H, -OH); 1.93 (p, 1 H, O-CH<sub>2</sub>-CH-); 0.90 (s, 9 H, Si-C(CH<sub>3</sub>)); 0.09 (s, 6 H, Si-CH<sub>3</sub>). <sup>13</sup>C NMR (500 MHz, CDCl<sub>3</sub>):  $\delta$  64.2 (s, 1 C, Si-O-CH<sub>2</sub>-); 63.6 (s, 2 C, -CH<sub>2</sub>-OH); 44.3 (s, 1 C, CH(CH<sub>2</sub>-O-)<sub>3</sub>); 26.0 (t, 3 C, Si-C(CH<sub>3</sub>)); 18.4 (s, 1 C, Si-C-(CH<sub>3</sub>)<sub>3</sub>); -5.4 (s, 2 C, Si-CH<sub>3</sub>).

**Synthesis of TBDMS-(PEG)<sub>2</sub>.** Preparation of TBDMS-(PEG)<sub>2</sub> was performed according to a previously published procedure with minor modifications.<sup>31</sup> 240 mg of KH (6 mmol, dispersed in mineral oil) was added into a round-bottom flask and then washed with anhydrous cyclohexane three times. The remaining cyclohexane was removed by applying vacuum. To the flask, freshly distilled THF was charged via vapor phase, and 550 mg of TBDMS-MPD (5 mmol -OH) was then added. The mixture was allowed to stir at room temperature overnight. 20 g of ethylene oxide (454 mmol) was condensed onto dibutylmagnesium, and the mixture was stirred in a dry ice bath for 2 h. The mixture was then degassed (freeze-pump-thaw cycles) three times, and the purified ethylene oxide was transferred in vacuo into the TBDMS-MPD/KH mixture. The reaction mixture was stirred at room temperature for 2 days. The polymerization was terminated by adding 2 mL of 5 wt % K<sub>2</sub>CO<sub>3</sub>, and the crude product was precipitated with hexane, ethyl ether, and methanol in succession. After drying, 15.0 g of TBDMS-(PEG)<sub>2</sub> was obtained in the form of a white powder. <sup>1</sup>H NMR (500 MHz, CDCl<sub>3</sub>):  $\delta$  3.78–3.48 (m, PEG -CH<sub>2</sub>-); 2.18 (br s, 1 H, -OH); 0.89 (s, 9 H, Si-C(CH<sub>3</sub>)); 0.06 (s, 6 H, Si-CH<sub>3</sub>). GPC-MALLS:  $\bar{M}_w$  = 8400,  $\bar{M}_w/\bar{M}_n$  = 1.13.

**Synthesis of TBDMS-(PEG-PLA)<sub>2</sub>.** 13.4 g of TBDMS-(PEG)<sub>2</sub> (3 mmol -OH) was dissolved in 100 mL of anhydrous THF. After adding 132 mg of 60% NaH (3.32 mmol NaH) in mineral oil, the mixture was stirred under Ar purging for 4 h. 1.72 g of lactide (12.0 mmol) was then added, and the polymerization was carried out under Ar for 2 days at room temperature. To terminate the reaction, 10 mL of 10% K<sub>2</sub>CO<sub>3</sub> and 100 mL of DCM were added and washed with saturated NaCl. The organic layer was quickly washed with an additional portion of saturated NaCl solution to prevent PLA degradation and dried over MgSO<sub>4</sub>. The organic solvent was then reduced, and the polymer was precipitated from ethyl ether and washed with ethyl ether and hexane. After drying, 9.90 g of TBDMS-(PEG-PLA)<sub>2</sub> was obtained. <sup>1</sup>H NMR (500 MHz, CDCl<sub>3</sub>):  $\delta$  5.25–5.16 (m, PLA -CH-); 4.22–4.23 (m, -CH<sub>2</sub>-O-C(=O)-); 4.10–3.43 (m, PEG -CH<sub>2</sub>-); 2.19 (t, 1 H, -Si-O-CH<sub>2</sub>-CH-(CH<sub>2</sub>-O-)<sub>2</sub>); 2.04 (br s, 1 H, -OH); 1.58–1.42

Scheme 2. Modification of G-PPM with DOPA (Reaction A), Oligo-(DOPA) (Reaction B), and Oligo-(DOPA-Lys) (Reaction C)



(m, PLA  $-\text{CH}_3$ ); 0.89 (s, 9 H, Si- $\text{C}(\text{CH}_3)_3$ ); 0.64 (s, 6 H, Si- $\text{CH}_3$ ).

**Synthesis of TBDMS-(PEG-PLA-MA)<sub>2</sub> (TBDMS-PPM).** 8.79 g of TBDMS-(PEG-PLA)<sub>2</sub> (1.97 mmol  $-\text{OH}$ ) was dissolved in 35 mL of chloroform. 1.25 mL of methacrylic anhydride (7.88 mmol) and 1.11 mL of triethylamine (7.88 mmol) were added, and the mixture was stirred at room temperature for 2 days. The crude polymer was precipitated by ethyl ether once and by cold methanol twice. After drying, 7.66 g of TBDMS-PPM was obtained. <sup>1</sup>H NMR (500 MHz, CDCl<sub>3</sub>):  $\delta$  6.21 (s, 1 H,  $\text{HHC}=\text{C}(\text{CH}_3)-\text{C}(\text{O})-\text{O}-$ ); 5.64 (s, 1 H,  $\text{HHC}=\text{C}(\text{CH}_3)-\text{C}(\text{O})-\text{O}-$ ); 5.25–5.16 (m, PLA  $-\text{CH}-$ ); 4.22–4.23 (m,  $-\text{CH}_2-\text{O}-\text{C}(\text{O})-$ ); 4.10–3.43 (m, PEG  $-\text{CH}_2-$ ); 2.19 (t, 1 H,  $-\text{Si}-\text{O}-\text{CH}_2-\text{CH}-(\text{CH}_2-\text{O}-)_2$ ); 1.97 (s, 3 H,  $\text{H}_2\text{C}=\text{C}(\text{CH}_3)-\text{C}(\text{O})-\text{O}-$ ); 1.58–1.25 (m, PLA  $-\text{CH}_3$ ); 0.89 (s, 9 H, Si- $\text{C}(\text{CH}_3)_3$ ); 0.63 (s, 6 H, Si- $\text{CH}_3$ ).

**Synthesis of HO-(PEG-PLA-MA)<sub>2</sub> (HO-PPM).** 7.62 g of TBDMS-PPM (0.837 mmol) was dissolved in 25 mL of chloroform and purged with Ar for 10 min. 37 mL of 4 M HCl in dioxane was added, and the mixture was stirred under Ar for 15 min. The volume of the solvent was then reduced through rotary evaporation, and the mixture was added to cold ethyl ether. The precipitate was vacuum-filtered and washed with ethyl ether and hexane. After drying, 7.27 g of HO-PPM was obtained. <sup>1</sup>H NMR (500 MHz, CDCl<sub>3</sub>):  $\delta$  6.21 (s, 1 H,  $\text{C}(\text{O})-\text{C}(\text{CH}_3)=\text{CHH}$ ); 5.64 (s, 1 H,  $\text{C}(\text{O})-\text{C}(\text{CH}_3)=\text{CHH}$ ); 5.25–5.13 (m, PLA  $\text{C}(\text{O})-\text{CH}(\text{CH}_3)-\text{O}$ ); 4.41–4.23 (m, PEG,  $\text{C}(\text{O})-\text{O}-\text{CH}_2$ ); 3.81–3.48 (m, PEG  $-\text{CH}_2-\text{O}$ ); 2.19 (t, 1 H,  $-\text{O}-\text{CH}_2-\text{CH}-(\text{CH}_2-\text{O}-)_2$ ); 2.13 (br s, 1 H,  $-\text{OH}$ ); 1.97 (s, 3 H,  $\text{C}(\text{O})-\text{C}(\text{CH}_3)=\text{CH}_2$ ); 1.70–1.43 (m, PLA  $\text{C}(\text{O})-\text{CH}(\text{CH}_3)-\text{O}$ ).

**Synthesis of *N*-Boc-Gly-(PEG-PLA-MA)<sub>2</sub> (BG-PPM).** 3 g of HO-PPM (0.33 mmol) was azeotropically dried with benzene and placed in a desiccator for 4 h. The block copolymer was then dissolved in 20 mL of anhydrous DCM and 20 mL of anhydrous DMF and purged with Ar for 10 min. 173 mg of *N*-Boc-Gly (0.99

mmol), 204 mg of DCC (0.99 mmol), and 4 mg of DMAP (0.033 mmol) were added, and the mixture was stirred at room temperature for 20 h. The product was purified by precipitating twice in ethyl ether and once in cold methanol. After drying, 2.58 g of BG-PPM was obtained. <sup>1</sup>H NMR (500 MHz, CDCl<sub>3</sub>):  $\delta$  6.21 (s, 1 H,  $\text{C}(\text{O})-\text{C}(\text{CH}_3)=\text{CHH}$ ); 5.64 (s, 1 H,  $\text{C}(\text{O})-\text{C}(\text{CH}_3)=\text{CHH}$ ); 5.25–5.14 (m, PLA  $\text{C}(\text{O})-\text{CH}(\text{CH}_3)-\text{O}$ ); 5.13 (s, 2 H,  $-\text{N}-\text{CH}_2-\text{C}(\text{O})-\text{O}$ ); 4.31 (br, PEG,  $\text{C}(\text{O})-\text{O}-\text{CH}_2$ ); 3.81–3.48 (m, PEG  $-\text{CH}_2-\text{O}$ ); 2.19 (t, 1 H,  $-\text{O}-\text{CH}_2-\text{CH}-(\text{CH}_2-\text{O}-)_2$ ); 1.97 (s, 3 H,  $\text{C}(\text{O})-\text{C}(\text{CH}_3)=\text{CH}_2$ ); 1.70–1.50 (m, PLA  $\text{C}(\text{O})-\text{CH}(\text{CH}_3)-\text{O}$ ); 1.45 (s, 9 H,  $(\text{CH}_3)_3\text{C}-\text{O}(\text{O})-\text{N}-$ ).

**Synthesis of H<sub>2</sub>N-Gly-(PEG-PLA-MA)<sub>2</sub> (G-PPM).** 2.58 g of BG-PPM was dissolved in 10 mL of chloroform, and then 15 mL of 4 M HCl in dioxane was added. The mixture was stirred at room temperature with Ar purging for 15 min. After rotary evaporation of HCl, the block copolymer was precipitated with ethyl ether and washed with hexane. 2.18 g of G-PPM was obtained after drying. <sup>1</sup>H NMR (500 MHz, DMSO-*d*<sub>6</sub>):  $\delta$  7.99 (s, br,  $-\text{NH}_2$ ); 6.10 (s, 1 H,  $\text{C}(\text{O})-\text{C}(\text{CH}_3)=\text{CHH}$ ); 5.77 (s, 1 H,  $\text{C}(\text{O})-\text{C}(\text{CH}_3)=\text{CHH}$ ); 5.25–5.13 (m, PLA  $\text{C}(\text{O})-\text{CH}(\text{CH}_3)-\text{O}$ ); 5.13 (s, 2 H,  $-\text{N}-\text{CH}_2-\text{C}(\text{O})-\text{O}$ ); 4.22 (br, PEG,  $\text{C}(\text{O})-\text{O}-\text{CH}_2$ ); 3.90–3.30 (m, PEG  $-\text{CH}_2-\text{O}$ ); 2.00 (t, 1 H,  $-\text{O}-\text{CH}_2-\text{CH}-(\text{CH}_2-\text{O}-)_2$ ); 1.89 (s, 3 H,  $\text{C}(\text{O})-\text{C}(\text{CH}_3)=\text{CH}_2$ ); 1.70–1.34 (m, PLA  $\text{C}(\text{O})-\text{CH}(\text{CH}_3)-\text{O}$ ).

**Synthesis of *N*-tert-Butyloxycarbonyl-3,4-dihydroxyphenylalanine (*N*-Boc-DOPA).** *N*-Boc-DOPA was synthesized as follows.<sup>30</sup> 135 mL of 0.4 M NaHCO<sub>3</sub> was bubbled with Ar for 20 min and then added 21.5 g of DOPA (108 mmol). 25 g of Boc<sub>2</sub>O (112 mmol) in 135 mL of THF was added, and the mixture was stirred with Ar bubbling for 20 h. After evaporating THF, the aqueous layer was washed with equal volume of ethyl ether. The pH of the aqueous layer was reduced to 7 by adding concentrated HCl and washed with equal volume of ethyl ether. These two ether layers were discarded while the aqueous layer was further acidified



to pH 2. The crude product was extracted from the acidified aqueous layer two more times with ethyl ether, and these organic layers were combined and dried over  $\text{MgSO}_4$ . After evaporating ethyl ether, the crude *N*-Boc-DOPA was further purified by column chromatography using a gradient methanol/chloroform eluting solvent. 18.3 g of *N*-Boc-DOPA was obtained after drying.  $^1\text{H}$  NMR (500 MHz,  $\text{DMSO}-d_6$ ):  $\delta$  6.93–6.63 (3 H,  $-\text{C}_6\text{H}_3(\text{OH})_2$ ); 3.99 (s, 1 H,  $-\text{N}-\text{CH}(\text{CH}_2)-\text{C}(=\text{O})-\text{OH}$ ); 2.90 (d, 1 H,  $-\text{CH}-\text{CHH}-\text{C}_6\text{H}_3(\text{OH})_2$ ); 2.73 (q, 1 H,  $-\text{CH}-\text{CHH}-\text{C}_6\text{H}_3(\text{OH})_2$ ); 1.33 (s, 9 H,  $(\text{CH}_3)_3\text{C}-\text{O}(\text{=O})-\text{N}-$ ).

**Synthesis of *N*-Boc-DOPA-Gly-(PEG-PLA-MA)<sub>2</sub> (BY-PPM).** 1.0 g of G-PPM (0.11 mmol) was dissolved in 14 mL of DCM and 7 mL of DMF, and 63 mg of *N*-Boc-DOPA (0.22 mmol), 56 mg of HOBt (0.37 mmol), 83 mg of HBTU (0.22 mmol), and 51  $\mu\text{L}$  of  $\text{Et}_3\text{N}$  (0.37 mmol) were added. The reaction mixture was stirred for 30 min at room temperature and precipitated by adding to ethyl ether. After further precipitation in methanol and ethyl ether, 950 mg of BY-PPM was obtained.  $^1\text{H}$  NMR (500 MHz,  $\text{DMSO}-d_6$ ):  $\delta$  6.93–6.50 (3 H,  $-\text{C}_6\text{H}_3(\text{OH})_2$ ); 6.10 (s, 1 H,  $\text{C}(=\text{O})-\text{C}(\text{CH}_3)=\text{CHH}$ ); 5.77 (s, 1 H,  $\text{C}(=\text{O})-\text{C}(\text{CH}_3)=\text{CHH}$ ); 5.24–5.15 (m, PLA  $\text{C}(=\text{O})-\text{CH}(\text{CH}_3)-\text{O}$ ); 5.10 (s, 2 H,  $-\text{N}-\text{CH}_2-\text{C}(=\text{O})-\text{O}$ ); 4.22 (s, 1 H,  $-\text{N}-\text{CH}(\text{CH}_2)-\text{C}(=\text{O})-\text{N}-$ ); 4.16 (PEG,  $\text{C}(=\text{O})-\text{O}-\text{CH}_2$ ); 3.81–3.48 (m, PEG  $-\text{CH}_2-\text{O}$ ); 2.79 (d, 1 H,  $-\text{CH}-\text{CHH}-\text{C}_6\text{H}_3(\text{OH})_2$ ); 2.70 (d, 1 H,  $-\text{CH}-\text{CHH}-\text{C}_6\text{H}_3(\text{OH})_2$ ); 2.00 (t, 1 H,  $-\text{O}-\text{CH}_2-\text{CH}-(\text{CH}_2-\text{O}-)_2$ ); 1.89 (s, 3 H,  $\text{C}(=\text{O})-\text{C}(\text{CH}_3)=\text{CH}_2$ ); 1.50–1.35 (m, PLA  $\text{C}(=\text{O})-\text{CH}(\text{CH}_3)-\text{O}$ ); 1.30 (s, 9 H,  $(\text{CH}_3)_3\text{C}-\text{O}(\text{=O})-\text{N}-$ ).

**Synthesis of DOPA-Gly-(PEG-PLA-MA)<sub>2</sub> (Y-PPM).** 500 mg of BY-PPM was dissolved in 2 mL of chloroform and purged with Ar for 10 min. 3 mL of 4 M HCl in dioxane was added, and the mixture was stirred for 15 min. After evaporating HCl, the mixture was added to ethyl ether and washed with hexane. 450 mg of Y-PPM was obtained after drying.  $^1\text{H}$  NMR (500 MHz,  $\text{DMSO}-d_6$ ):  $\delta$  6.66 (s, 2 H,  $-\text{C}_6\text{H}_2(\text{OH})_2$ ); 6.52 (d, 1 H,  $\text{C}_6\text{H}_2\text{H}(\text{OH})_2-$ ); 6.10 (s, 1 H,  $\text{C}(=\text{O})-\text{C}(\text{CH}_3)=\text{CHH}$ ); 5.77 (s, 1 H,  $\text{C}(=\text{O})-\text{C}(\text{CH}_3)=\text{CHH}$ ); 5.24–5.15 (m, PLA  $\text{C}(=\text{O})-\text{CH}(\text{CH}_3)-\text{O}$ ); 5.10 (s, 2 H,  $-\text{N}-\text{CH}_2-\text{C}(=\text{O})-\text{O}$ ); 4.22 (s, 1 H,  $-\text{N}-\text{CH}(\text{CH}_2)-\text{C}(=\text{O})-\text{N}-$ ); 4.16 (PEG,  $\text{C}(=\text{O})-\text{O}-\text{CH}_2$ ); 3.81–3.48 (m, PEG  $-\text{CH}_2-\text{O}$ ); 2.95 (d, 1 H,  $-\text{CH}-\text{CHH}-\text{C}_6\text{H}_3(\text{OH})_2$ ); 2.69 (d, 1 H,  $-\text{CH}-\text{CHH}-\text{C}_6\text{H}_3(\text{OH})_2$ ); 2.01 (t, 1 H,  $-\text{O}-\text{CH}_2-\text{CH}-(\text{CH}_2-\text{O}-)_2$ ); 1.89 (s, 3 H,  $\text{C}(=\text{O})-\text{C}(\text{CH}_3)=\text{CH}_2$ ); 1.50–1.30 (m, PLA  $\text{C}(=\text{O})-\text{CH}(\text{CH}_3)-\text{O}$ ).

**General Procedure for NCA Polymerization.** G-PPM was first dried by azeotropic evaporation with benzene and placed in a desiccator to dry for at least 3 h. Ring-opening polymerization of NCA was performed by dissolving G-PPM in anhydrous THF at 100 mg/mL under argon. An equimolar amount of DIPEA was then added to the polymer solution. A 6 M excess of diacetyl-DOPA-NCA with or without Fmoc-Lys-NCA (equimolar to DOPA) was dissolved in anhydrous THF at 20 mg/mL and slowly added to the block copolymer mixture. The reaction mixture was stirred at room temperature for 2–5 days with a dry tube outlet. The peptide-modified block copolymers were purified in succession with ethyl ether, cold methanol, and ethyl ether. After drying,  $\text{Ac}_2\text{Y5-PPM}$ ,  $(\text{Ac}_2\text{Y3-FmocK2})\text{-PPM}$ , or  $(\text{Ac}_2\text{Y5-FmocK5})\text{-PPM}$  was obtained.

$\text{Ac}_2\text{Y5-PPM}$ :  $^1\text{H}$  NMR (500 MHz,  $\text{DMSO}-d_6$ ):  $\delta$  7.25–7.01 (m,  $-\text{C}_6\text{H}_3(\text{OH})_2$ ); 6.10 (s, 1 H,  $\text{C}(=\text{O})-\text{C}(\text{CH}_3)=\text{CHH}$ ); 5.78 (s, 1 H,  $\text{C}(=\text{O})-\text{C}(\text{CH}_3)=\text{CHH}$ ); 5.25–5.10 (m, PLA,  $\text{C}(=\text{O})-\text{CH}(\text{CH}_3)-\text{O}$ ); 5.10 (s, 2 H,  $-\text{N}-\text{CH}_2-\text{C}(=\text{O})-\text{O}$ ); 4.35 (br,  $-\text{NH}-\text{CH}(\text{CH}_2)-\text{C}(=\text{O})-$ ); 4.18 (PEG,  $\text{C}(=\text{O})-\text{O}-\text{CH}_2$ ); 4.00–3.31 (m, PEG  $-\text{CH}_2-\text{O}$ ); 2.98 (br,  $-\text{CH}-\text{CH}_2-\text{C}_6\text{H}_3(\text{OH})_2$ ); 2.18 (d,  $-\text{O}-\text{C}(=\text{O})-\text{CH}_3$ ); 2.01 (t, 1 H,  $-\text{O}-\text{CH}_2-\text{CH}-(\text{CH}_2-\text{O}-)_2$ ); 1.89 (s, 3 H,  $\text{C}(=\text{O})-\text{C}(\text{CH}_3)=\text{CH}_2$ ); 1.50–1.25 (m, PLA  $\text{C}(=\text{O})-\text{CH}(\text{CH}_3)-\text{O}$ ).

$(\text{Ac}_2\text{Y3-FmocK2})\text{-PPM}$  and  $(\text{Ac}_2\text{Y5-FmocK5})\text{-PPM}$ :  $^1\text{H}$  NMR (500 MHz,  $\text{DMSO}-d$ ):  $\delta$  7.90–7.29 (m, 8 H, Fmoc benzyl  $-\text{CH}-$ ); 7.25–7.01 (m,  $-\text{C}_6\text{H}_3(\text{OH})_2$ ); 6.10 (s, 1 H,  $\text{C}(=\text{O})-\text{C}(\text{CH}_3)=\text{CHH}$ ); 5.77 (s, 1 H,  $\text{C}(=\text{O})-\text{C}(\text{CH}_3)=\text{CHH}$ ); 5.25–5.10 (m, PLA,  $\text{C}(=\text{O})-\text{CH}(\text{CH}_3)-\text{O}$ ); 5.10 (s, 2 H,  $-\text{N}-\text{CH}_2-\text{C}(=\text{O})-\text{O}$ ); 4.55 (br,  $-\text{NH}-\text{CH}(\text{CH}_2)-\text{C}(=\text{O})-$ ); 4.29 (d, Fmoc,  $-\text{C}(=\text{O})-\text{O}-\text{CH}_2-\text{CH}-$ ); 4.22 (Fmoc,  $-\text{C}(=\text{O})-\text{O}-\text{CH}_2-\text{CH}-$ ); 4.18 (PEG,

$\text{C}(=\text{O})-\text{O}-\text{CH}_2$ ); 4.00–3.31 (m, PEG  $-\text{CH}_2-\text{O}$ ); 2.98 (br,  $-\text{CH}-\text{CHH}-\text{C}_6\text{H}_3(\text{OH})_2$ ); 2.92 (s, Lys,  $-(\text{CH}_2)_3-\text{CH}_2-\text{NH}-\text{CO}_2-$ ); 2.74 (br,  $-\text{CH}-\text{CHH}-\text{C}_6\text{H}_3(\text{OH})_2$ ); 2.16 (d,  $-\text{O}-\text{C}(=\text{O})-\text{CH}_3$ ); 2.00 (t, 1 H,  $-\text{O}-\text{CH}_2-\text{CH}-(\text{CH}_2-\text{O}-)_2$ ); 1.89 (s, 3 H,  $\text{C}(=\text{O})-\text{C}(\text{CH}_3)=\text{CH}_2$ ); 1.70–1.08 (m,  $-\text{CH}-(\text{CH}_2)_3-\text{CH}_2-\text{NH}-$ ); 1.50–1.25 (m, PLA  $\text{C}(=\text{O})-\text{CH}(\text{CH}_3)-\text{O}$ ).

**Deprotection of Peptide Side Chain.** Protected polymer ( $\text{Ac}_2\text{Y5-PPM}$ ,  $(\text{Ac}_2\text{Y3-FmocK2})\text{-PPM}$ , or  $(\text{Ac}_2\text{Y5-FmocK5})\text{-PPM}$ ) was dissolved in anhydrous DMF at a concentration of 50 mg/mL and bubbled with Ar for 10 min. Pyridine was added to make a 5% solution and stirred for 15 min with Ar bubbling. The mixture was rotary-evaporated to remove excess pyridine and added to ethyl ether to obtain Y5-PPM, Y3K2-PPM, or Y5K5-PPM. The precipitated solid was placed in the desiccator to dry for at least 3 days.

Y5-PPM:  $^1\text{H}$  NMR (500 MHz,  $\text{DMSO}-d_6$ ):  $\delta$  6.68–6.42 (m,  $-\text{C}_6\text{H}_3(\text{OH})_2$ ); 6.10 (s, 1 H,  $\text{C}(=\text{O})-\text{C}(\text{CH}_3)=\text{CHH}$ ); 5.78 (s, 1 H,  $\text{C}(=\text{O})-\text{C}(\text{CH}_3)=\text{CHH}$ ); 5.25–5.10 (m, PLA,  $\text{C}(=\text{O})-\text{CH}(\text{CH}_3)-\text{O}$ ); 5.10 (s, 2 H,  $-\text{N}-\text{CH}_2-\text{C}(=\text{O})-\text{O}$ ); 4.35 (br,  $-\text{NH}-\text{CH}(\text{CH}_2)-\text{C}(=\text{O})-$ ); 4.18 (PEG,  $\text{C}(=\text{O})-\text{O}-\text{CH}_2$ ); 4.00–3.31 (m, PEG  $-\text{CH}_2-\text{O}$ ); 2.79 (br,  $-\text{CH}-\text{CH}_2-\text{C}_6\text{H}_3(\text{OH})_2$ ); 2.01 (t, 1 H,  $-\text{O}-\text{CH}_2-\text{CH}-(\text{CH}_2-\text{O}-)_2$ ); 1.89 (s, 3 H,  $\text{C}(=\text{O})-\text{C}(\text{CH}_3)=\text{CH}_2$ ); 1.50–1.25 (m, PLA  $\text{C}(=\text{O})-\text{CH}(\text{CH}_3)-\text{O}$ ).

Y3K2-PPM and Y5K5-PPM:  $^1\text{H}$  NMR (500 MHz,  $\text{DMSO}-d$ ):  $\delta$  6.68–6.42 (m,  $-\text{C}_6\text{H}_3(\text{OH})_2$ ); 6.10 (s, 1 H,  $\text{C}(=\text{O})-\text{C}(\text{CH}_3)=\text{CHH}$ ); 5.77 (s, 1 H,  $\text{C}(=\text{O})-\text{C}(\text{CH}_3)=\text{CHH}$ ); 5.23–5.10 (m, PLA,  $\text{C}(=\text{O})-\text{CH}(\text{CH}_3)-\text{O}$ ); 5.13 (s, 2 H,  $-\text{N}-\text{CH}_2-\text{C}(=\text{O})-\text{O}$ ); 4.40 (br,  $-\text{NH}-\text{CH}(\text{CH}_2)_4-\text{C}(=\text{O})-$ ); 4.34 (br,  $-\text{NH}-\text{CH}(\text{CH}_2)-\text{C}_6\text{H}_3-$ ); 4.35 (br,  $-\text{NH}-\text{CH}(\text{CH}_2)-\text{C}(=\text{O})-$ ); 4.17 (PEG,  $\text{C}(=\text{O})-\text{O}-\text{CH}_2$ ); 4.00–3.20 (m, PEG  $-\text{CH}_2-\text{O}$ ); 2.98 (br,  $-\text{CH}-\text{CHH}-\text{C}_6\text{H}_3(\text{OH})_2$ ); 2.76 (s,  $-(\text{CH}_2)_3-\text{CH}_2-\text{NH}_2$ ); 2.74 (br,  $-\text{CH}-\text{CHH}-\text{C}_6\text{H}_3(\text{OH})_2$ ); 2.00 (t, 1 H,  $-\text{O}-\text{CH}_2-\text{CH}-(\text{CH}_2-\text{O}-)_2$ ); 1.89 (s, 3 H,  $\text{C}(=\text{O})-\text{C}(\text{CH}_3)=\text{CH}_2$ ); 1.79–1.10 (m,  $-\text{CH}-(\text{CH}_2)_3-\text{CH}_2-\text{NH}-$ ); 1.50–1.25 (m, PLA  $\text{C}(=\text{O})-\text{CH}(\text{CH}_3)-\text{O}$ ).

**Molecular Weight Analysis.** Molecular weights were determined by GPC-MALLS on a DAWN EOS (Wyatt Technology) using Shodex-OH Pak columns in an aqueous mobile phase (50 mM phosphate buffered saline (PBS), 0.1 M NaCl, 0.05%  $\text{NaN}_3$ ; pH = 6.0) and a Optilab DSP (Wyatt Technology) refractive index detector. For molecular weight calculations, the experimentally determined  $dn/dc$  value of mPEG-NH<sub>2</sub> (MW 5000, 0.136) was used.<sup>13</sup>

**Quantification of DOPA Content.** The DOPA content of the block copolymers was determined using UV absorbance of polymer solutions in 12.1 mM HCl at the maximum absorbance wavelength of the catechol ( $\lambda_{\text{max}} = 280$  nm). Solutions containing known concentrations of free DOPA amino acid were used to construct the calibration curve.

**Photopolymerization.** The block copolymers were dissolved in 10 mM HEPES buffer in 150 mM NaCl (pH 7.4) that was previously bubbled with  $\text{N}_2$ . DMPA (120 mg/mL in VP) was added to make the precursor solution with the final polymer concentration of 150 mg/mL and 9.4 mM DMPA. 50  $\mu\text{L}$  of the precursor solution was pipetted onto a glass slide treated with 1H,1H,2H,2H-perfluorooctyltrichlorosilane and irradiated for up to 1 min with a handheld UV lamp (Black Ray lamp, 365 nm, model UVL-56, UVP, CA).

**Contact Mechanics Test.** Contact mechanics testing was performed as described previously<sup>16</sup> on hemispherical photocured hydrogels to characterize their mechanical and adhesive properties. Polymer precursor solutions were irradiated for 10 min in a  $\text{N}_2$ -rich glovebag to ensure complete photopolymerization at the surface of the hemispherical gels. Photocured hydrogels were placed in HEPES buffer for at least 1 h prior to testing to ensure equilibrium swelling conditions. Preliminary experiments showed that swelling of the hydrogels was complete within 1 h under these conditions (data not shown). To preserve the reduced form of DOPA, the hydrogels were kept in a  $\text{N}_2$ -rich chamber until testing. All tests were performed within 4 h of gel preparation to avoid the effects of polymer degradation. A photo of each hemispherical gel was taken, and the height and the base of the hydrogels were used to determine the radius of curvature of the contacting surface. To test

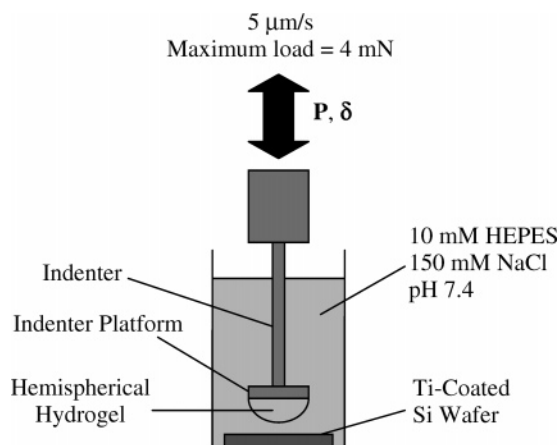


**Figure 1.** Contact mechanics experimental setup.

the effect of oxidation on the adhesive interaction between DOPA and Ti, a group of DOPA-containing gels were submerged in a buffer containing 10 mM NaIO<sub>4</sub>, 10 mM HEPES, and 150 mM NaCl (pH 7.4) for 10 min and then extracted with the HEPES buffer for at least 30 min prior to mechanical testing.

The surface to which hydrogels were adhered consisted of 80 mm × 80 mm pieces of Si wafer coated with 20 nm of Ti through electron-beam evaporation. [Note: although we refer to these substrates as Ti throughout this paper, it should be understood that the surface to which the hydrogel makes contact is a titanium oxide as was confirmed using X-ray photoelectron spectroscopy (data not shown).] The Ti surfaces were cleaned by sonication in 5% Contrad 70 solution, deionized water, acetone, and hexane before they were adhered to the bottom of a glass vial (outer diameter = 19 mm, height = 50 mm) using superglue and dried in a vacuum for at least 2 days. Just before mechanical testing, the surfaces were sonicated twice in propanol and cleaned with O<sub>2</sub> plasma.

Adhesion experiments were performed using the testing apparatus shown in Figure 1. Hemispherical gel caps were attached to the platform (diameter = 6.3 mm) of an indenter (diameter = 0.9 mm) using superglue. The other end of the indenter was attached to a piezoelectric stepping motor (IW-701-00, Burleigh Instruments, NY) aligned in series with a 50 g load transducer (FTD-G-50, Schaevitz Sensors, VA) with a resolution of ~0.1 mN. A fiber-optic displacement sensor (RC100-GM2OV, Philtec, Inc., MD) was used to measure the axial movement of the steel rod. The glass vial containing the Ti-coated Si wafer was positioned below the hydrogel and flooded with HEPES buffer to test the adhesive interaction in an aqueous environment. The indenter was advanced at 5 μm/s until a maximum compressive load of 4 mN was measured, and then the indenter was retracted at the same speed until the hydrogel had fully detached from the surface. Load and displacement values were recorded throughout the experiment.

**Statistical Analysis.** A minimum of five samples of each hydrogel were tested as described above. Statistical analysis was performed using analysis of variance (ANOVA) and Tukey post hoc analysis using a significance level of  $p = 0.05$ .

## Results

As illustrated in Scheme 1, synthesis of G-PPM was accomplished by first protecting one of the three hydroxyl groups in 2-hydroxymethylpropane-1,3-diol (HMPD) with TBDMS to make TBDMS-MPD, which was used as an initiator for anionic ring-opening polymerization of ethylene oxide. The resulting two-tailed TBDMS-(PEG)<sub>2</sub> (GPC-MALLS  $\bar{M}_w = 8400$ ;  $\bar{M}_w/\bar{M}_n = 1.13$ ) was further reacted with L-lactide (LA) monomers through anionic ring-opening polymerization to prepare TBDMS-(PEG-PLA)<sub>2</sub>. The average length of LA repeat units in TBDMS-(PEG-PLA)<sub>2</sub> was found to be 5.2 based on <sup>1</sup>H NMR integral values of PEG at  $\delta$  4.10–3.42 and PLA at  $\delta$  1.58–1.42. HO-PPM was then prepared by end-capping the PLA

**Table 1.** Amino Acid Composition of Synthesized Block Copolymers

samples	no. of amino acid residues per block copolymer			
	DOPA		Lys	
	<sup>1</sup> H NMR DMSO- <i>d</i> <sub>6</sub>	ABS 280 nm	<sup>1</sup> H NMR DMSO- <i>d</i> <sub>6</sub>	DOPA (wt %) <sup>a</sup>
Y-PPM	0.83	0.91 ± 0.084		2.0 ± 0.16
Y5-PPM	5.1	5.4 ± 0.29		10 ± 0.51
Y3K2-PPM	3.2	3.6 ± 0.57	2.4	6.9 ± 1.0
Y5K5-PPM	4.7	5.2 ± 1.1	5.1	9.0 ± 1.9

<sup>a</sup> Calculated from absorbance at 280 nm.

terminal hydroxyl groups with methacrylate and removing the TBDMS protecting group using 2.4 N HCl. Finally, the free –OH group was modified with *N*-Boc-Gly, and after deprotection of Boc, the building block G-PPM was obtained.

G-PPM was used to synthesize several DOPA-containing block copolymers (Scheme 2). To modify the block copolymer with a single DOPA (Scheme 2, reaction A), G-PPM was reacted with *N*-Boc-DOPA using carbodiimide chemistry. Subsequent removal of Boc was achieved by HCl treatment to obtain Y-PPM. DOPA functionalization was verified with <sup>1</sup>H NMR and UV–vis spectroscopy, and it was determined that over 83% of the block copolymers were functionalized with DOPA, as shown in Table 1.

To modify the amphiphilic block copolymer with oligomeric DOPA-containing peptides, the primary amine of G-PPM was used to initiate polymerization of diacetyl-DOPA-NCA and Fmoc-Lys-NCA to form Y5-PPM, Y3K2-PPM, and Y5K5-PPM (Scheme 2, reactions B and C). The length and composition of the peptide were controlled by the G-PPM:NCA reaction stoichiometry as well as the length of reaction time. Deprotection of the diacetyl-DOPA and Fmoc-Lys residues was performed without hydrolyzing the polyester groups, as <sup>1</sup>H NMR integral values of PLA and methacrylate peaks did not decrease after treatment with 5% pyridine for 15 min. The number of polymer-bound DOPA or Lys residues was determined by <sup>1</sup>H NMR (DOPA: phenyl peaks  $\delta$  6.68–6.42; Lys:  $-(CH_2)_3-$  peaks at 1.73–1.28 ppm), and the DOPA content was further confirmed by monitoring the absorbance of the catechol at its  $\lambda_{max}$  of 280 nm (Table 1). As many as five DOPA and five Lys residues were anchored onto the photocurable block copolymer, resulting in DOPA contents as high as 10 wt %. In the gelation and adhesion studies to be described below, DOPA-containing hydrogels were compared against DOPA-free control gels fabricated in an identical manner from HO-PPM copolymer.

All synthesized block copolymers were highly water-soluble, and buffered polymer solutions (15 wt % polymer) were photocured into hydrogels using DMPA as the photoinitiator and long wavelength UV, with gelation occurring in as little as 20 s of UV irradiation. VP was used as a solvent for the hydrophobic DMPA, and it is copolymerized with terminal methacrylate groups during the photopolymerization process.<sup>1</sup> Photopolymerization was performed in the presence of atmospheric oxygen, and DOPA-functionalized block copolymers initially retained an uncured liquid surface layer, which disappeared with UV exposure longer than 3 min. DOPA content had no apparent effect on the gelation process, as polymers with no, low, and high DOPA content gelled in comparable times under identical illumination conditions.

Adhesion of DOPA-containing hydrogels in contact with Ti was measured by the JKR method.<sup>32</sup> Ti was chosen as the surface to be tested since it is commonly used in medical alloys, and the interaction between titanium oxides and catechols has been well documented in the literature.<sup>14,18,33–35</sup> In our experi-

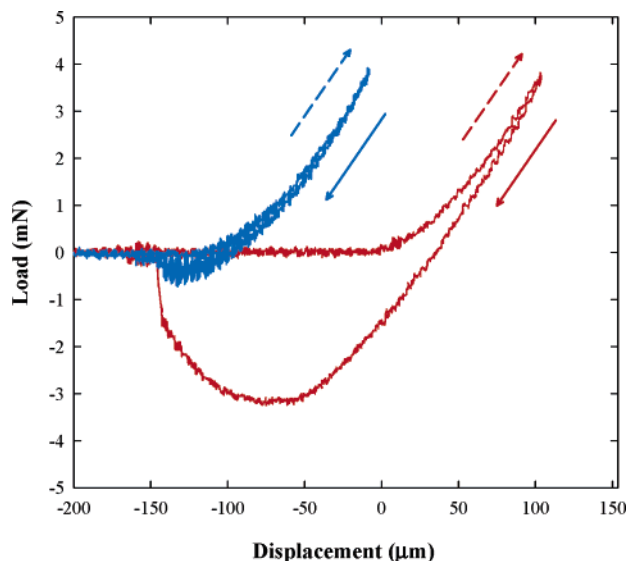


**Figure 2.** Representative load vs displacement curves of HO-PPM (blue curve) and  $\underline{\text{Y5}}$ -PPM (red curve) gels contacting Ti-coated Si wafer submerged in aqueous buffer. Dashed arrows indicate the advancing (indentation) portion of the curve, whereas the solid arrows indicate the receding (pull-off) portion of the contact curve.

**Table 2. Young's Modulus of DOPA-Modified Block Copolymer Gels**

	Young's modulus (kPa)		Young's modulus (kPa)
HO-PPM	22.6 ± 3.05	$\underline{\text{Y3K2}}$ -PPM	31.3 ± 4.30
$\underline{\text{Y}}$ -PPM	42.4 ± 9.11 <sup>b</sup>	$\underline{\text{Y5K5}}$ -PPM	31.3 ± 3.58
$\underline{\text{Y5}}$ -PPM	36.1 ± 2.39 <sup>a</sup>		

<sup>a</sup>  $p < 0.05$ . <sup>b</sup>  $p < 0.001$  relative to HO-PPM.

ments, a photocured polymer hydrogel in a hemispherical form was brought into contact with a Ti surface immersed in aqueous buffer and then indented to a maximum load of 4 mN, after which it was retracted at the same rate until the surfaces were separated. Typical load vs displacement curves for hemispherical hydrogels contacting Ti substrates are shown in Figure 2. Young's modulus of the gels was obtained by fitting the advancing portion of load ( $P$ ) vs displacement ( $\delta$ ) data with eq 1:<sup>36</sup>

$$P = \frac{16R^{1/2}E}{9} \delta^{3/2} \quad (1)$$

where  $R$  is the radius of curvature determined by the height ( $h$ ) and base radius ( $r$ ) of each hydrogel using the following equation:<sup>37</sup>

$$R = \frac{h}{2} + \frac{r^2}{2h} \quad (2)$$

In all cases, the experimental load vs displacement data were well fitted ( $R > 0.99$ ) with eq 1.

Young's modulus for the block copolymer gels cured for 10 min with UV irradiation averaged around 20–40 kPa (Table 2). Similar modulus values were obtained for gels that were cured with just 1 min of UV exposure in the presence of atmospheric oxygen (data not shown), suggesting that the bulk of the gels were fully cured within a very short irradiation time. Both  $\underline{\text{Y}}$ -PPM and  $\underline{\text{Y5}}$ -PPM gels had modulus values that were significantly higher than that of the control (HO-PPM) gels.

Load vs displacement data were also used in determining the work of adhesion ( $W_{\text{adh}}$ ) between DOPA-functionalized hydro-

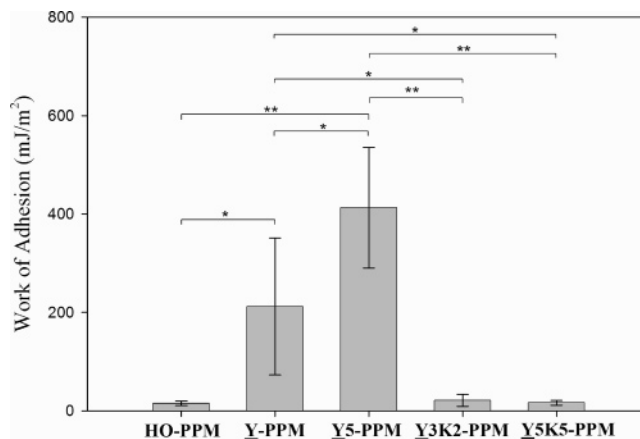


**Figure 3.** Work of adhesion for DOPA-modified block copolymer gels and contacting submerged Ti substrates. \*,  $p < 0.05$ ; \*\*,  $p < 0.001$ .

gels and Ti substrates. Contact curves (Figure 2) of HO-PPM gels showed little hysteresis, suggesting very little adhesion to the Ti surfaces. On the other hand, hydrogels consisting of  $\underline{\text{Y}}$ -PPM and  $\underline{\text{Y5}}$ -PPM showed large hysteresis between advancing and receding curves, indicating strong interactions between DOPA-modified gels and the metal oxide surface. To quantify the energy needed to separate DOPA-functionalized hydrogels from Ti surfaces, the overall work of adhesion was determined by integrating the measured load with respect to the displacement and normalizing this value by the maximum contact area ( $A_{\text{max}}$ ), as indicated in eq 3:<sup>38</sup>

$$W_{\text{adh}} = \frac{\int P d\delta}{A_{\text{max}}} \quad (3)$$

Although the contact area was not measured experimentally, it can be determined by fitting the advancing portions of the load vs displacement data with a Hertzian model in which the nonadhesive relationship between displacement and contact radius ( $a$ ) is given by<sup>36</sup>

$$\delta = \frac{a^2}{R} \quad (4)$$

$A_{\text{max}}$  is then calculated from  $a$  at the maximum  $\delta$ .

The average work of adhesion needed to separate block copolymer gels from Ti substrates submerged in HEPES buffer is shown in Figure 3. Hydrogels consisting of HO-PPM showed weak adhesion toward Ti surfaces ( $22.6 \pm 3.05$  mJ/m<sup>2</sup>). On the other hand, hydrogels modified with either a single DOPA or a short poly(DOPA) peptide showed significantly higher  $W_{\text{adh}}$  values.  $W_{\text{adh}}$  increased with increasing DOPA content in the gel network, as  $W_{\text{adh}}$  of  $\underline{\text{Y5}}$ -PPM gels ( $413 \pm 123$  mJ/m<sup>2</sup>) was roughly twice as much as  $\underline{\text{Y}}$ -PPM hydrogels ( $212 \pm 139$  mJ/m<sup>2</sup>). Surprisingly, gels modified with both DOPA and Lys did not show increased  $W_{\text{adh}}$  toward Ti surfaces as compared to HO-PPM.

To study the effect of DOPA oxidation on adhesion,  $\underline{\text{Y}}$ -PPM and control (HO-PPM) gels were treated with NaIO<sub>4</sub> for 10 min before the contact mechanics test was performed. Treatment of NaIO<sub>4</sub> did not affect the measured moduli of these hydrogels (Table 3). The appearance of HO-PPM gels remained unchanged after NaIO<sub>4</sub> treatment, whereas  $\underline{\text{Y}}$ -PPM gels turned red-orange instantly when submerged in 10 mM NaIO<sub>4</sub> solution, which indicated the oxidation of catechols. The  $W_{\text{adh}}$  of HO-PPM gels was not changed by NaIO<sub>4</sub> treatment; however,  $W_{\text{adh}}$



**Table 3. Young's Modulus of DOPA-Modified Block Copolymer Gels before and after NaIO<sub>4</sub> Treatment**

	Young's modulus (kPa)	
	untreated	NaIO <sub>4</sub> -treated
HO-PPM	22.6 ± 3.05	24.3 ± 2.58
Y-PPM	42.4 ± 9.11 <sup>a</sup>	54.6 ± 16.6 <sup>b</sup>

<sup>a</sup>  $p < 0.05$ . <sup>b</sup>  $p < 0.001$  relative to HO-PPM gels before and after NaIO<sub>4</sub> treatment.

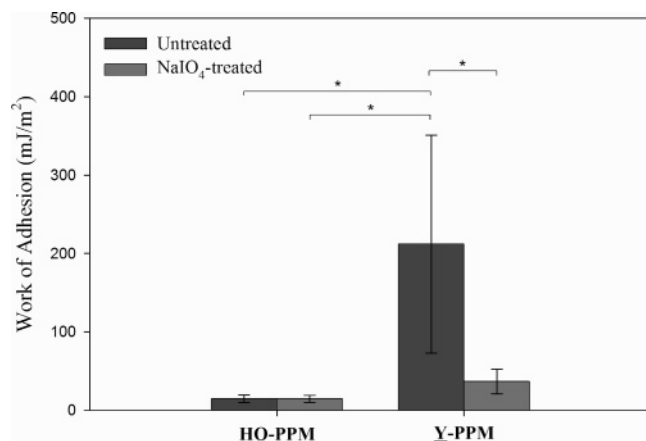


**Figure 4.** Effect of DOPA oxidation on work of adhesion for DOPA-modified block copolymer gels contacting submerged Ti substrates. \*,  $p < 0.01$ .

between Y-PPM gels and Ti was significantly reduced after NaIO<sub>4</sub> treatment (Figure 4), demonstrating that oxidation of DOPA reduces adhesion to metal oxide surfaces.

## Discussion

In the marine environment, polyphenolic mussel adhesive proteins (MAPs) are secreted by mussels for anchorage to surfaces in a wet, saline, and turbulent environment.<sup>39,40</sup> DOPA arises in MAPs due to post-translational modification of tyrosine in the presence of enzymes such as tyrosine hydroxylase.<sup>39</sup> MAPs isolated near the interface between the adhesive plaque and substratum (*Mytilus edulis* foot protein-3 (Mefp-3) and Mefp-5)<sup>41,42</sup> contain as much as 27 mol % DOPA and also high concentrations of basic residues such as lysine. Although the role of DOPA is not fully understood, a current hypothesis holds that the catecholic residue is important for water resistant adhesion and that oxidation of DOPA leads to intermolecular cross-link formation that results in the hardening of the adhesive plaques.<sup>43</sup>

The polymers synthesized in this study were designed to (1) rapidly form hydrogels by photopolymerization of the methacrylate end groups, (2) be biodegradable by virtue of the hydrolyzable PLA segments, and (3) contain DOPA for enhancement of adhesive properties of the resulting hydrogels. As our earlier work demonstrated,<sup>16</sup> incorporating DOPA into a gel by free radical polymerization is problematic due to radical quenching by the catechol side chain of DOPA.<sup>19–22</sup> To solve this problem, we employed elements of the block copolymer design used by Hubbell and co-workers, who developed a family of degradable ABA block copolymers composed of a central hydrophilic PEG block flanked by hydrophobic polyester domains terminated by methacrylate groups.<sup>1</sup> Aqueous solutions of these polymers photopolymerize in only a few seconds, a very desirable characteristic in a tissue sealant or adhesive. It has been speculated that the reason for such rapid gelation is due to the high effective concentration of the methacrylate

groups within the hydrophobic domains, leading to rapid propagation of the free-radical polymerization reaction.<sup>1</sup>

An important new feature that we have introduced in our block copolymers is the amine group of G-PPM, located midway along the hydrophilic PEG block (Scheme 1). This amine group provided a convenient location for modification of the hydrophilic PEG domain of the block copolymer with DOPA peptides of desired composition and length. DOPA modification was accomplished by either simple peptide coupling chemistry or NCA polymerization of short oligo-(DOPA) or oligo-(DOPA-Lys) peptides from the free amine group of G-PPM (Scheme 2). In Y3K2-PPM and Y5K5-PPM, Lys was incorporated into the oligopeptide to directly mimic Mefp-5. Mefp-5 has the highest DOPA content of all known MAPs, and the majority of Lys residues are located immediately adjacent to DOPA.<sup>42</sup> The presence of Lys may aid in substrate binding through electrostatic or hydrogen-bonding interactions. The final DOPA contents of Y5-PPM, Y3K2-PPM, and Y5K5-PPM were determined to be 10, 6.9, and 9.0 wt %, respectively (Table 1). It should be noted that these values are all less than Mefp-1 (~15 wt %) and considerably lower than the DOPA content in Mefp-3 and Mefp-5.<sup>41,42</sup>

Aqueous solutions of the block copolymers polymerized in less than 1 min under UV irradiation, yielding rigid gels with moduli between approximately 20 and 40 kPa. The design of the block copolymer, in which DOPA residues are located within the hydrophilic PEG block, ensures that when hydrated the DOPA will be located within the aqueous phase, thus limiting the inhibitive effect of the catechol on free-radical polymerization of methacrylate groups in the hydrophobic micelle core. The rapid gelation times of all DOPA-containing block copolymers demonstrate that interference by DOPA residues in the free radical polymerization was minimal. Slight retardation of polymerization observed at the hydrogel surface is likely due to the retarding effect of molecular oxygen.<sup>44</sup>

The placement of adhesive peptides midway along the hydrophilic PEG segment was expected to facilitate adhesive interactions between hydrogel-bound DOPA residues and tissue/implant surfaces, as illustrated schematically in Figure 5. To test this, we measured  $W_{adh}$  between our block copolymer hydrogels and Ti using the JKR method. JKR-based experiments have often been used to characterize interfacial binding energy between elastomeric gels in contact with a solid surface.<sup>38,45–47</sup> Most of the contact mechanics experiments reported in the literature have been carried out primarily in air, and only a few experiments have actually been performed surrounded by aqueous media.<sup>48,49</sup> Although more difficult to perform, adhesion tests performed in water are more relevant to the aqueous physiologic environment and eliminate weak nonspecific interactions (i.e., van der Waals) and capillary force interactions, the latter of which can be substantial considering that the surface energy of water is relatively high (72 mJ/m<sup>2</sup>).<sup>37</sup>

The effect of DOPA in enhancing hydrogel adhesion was apparent when present as a single DOPA residue (Y-PPM) or as an oligopeptide (Y5-PPM).  $W_{adh}$  of Y-PPM and Y5-PPM were found to be approximately 10 and 20 times greater than DOPA-free control gels (HO-PPM), respectively. These values are several orders of magnitude greater than  $W_{adh}$  of bioadhesive interactions in extracellular matrix (ECM) ligand–integrin binding<sup>48</sup> as well as adhesion between a synthetic polymer scaffold and hyaluronic acid, an ECM component of cartilage.<sup>49</sup> The measured Y-PPM and Y5-PPM gel–Ti  $W_{adh}$  values are also significantly stronger than nonspecific protein adsorption onto TiO<sub>2</sub> (50–80 mJ/m<sup>2</sup>) as determined by contact angle measure-

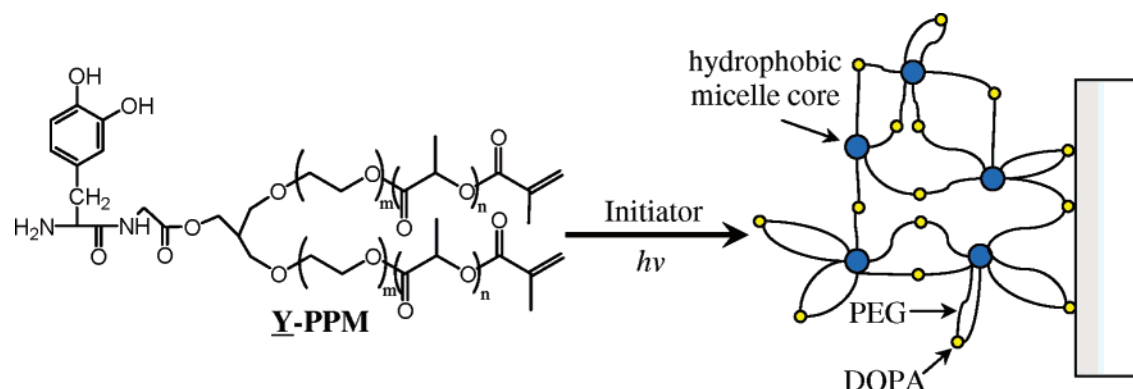


**Figure 5.** Illustrative schematic of photopolymerization of Y-PPM into an adhesive hydrogel.

ment<sup>50</sup> or atomic force microscopy (AFM).<sup>51</sup> As for MAP mimetic polymers, Yamamoto and colleagues reported work of adhesion values for synthetic polypeptides adsorbed onto various surfaces to be in the range 15–140 mJ/m<sup>2</sup>.<sup>52–54</sup>

Surprisingly, hydrogels formed from copolymers containing both DOPA and Lys (Y3K2-PPM and Y5K5-PPM) did not exhibit greater adhesion to Ti substrates than control hydrogels (Figure 3). Although the reasons for this are as yet unclear, one possible explanation for this could be poor presentation of poly-(DOPA-Lys) peptides on the surface of the gel. Since the gel surface is formed by photocuring the polymer precursor solution in air, partitioning of the more hydrophilic Lys-containing peptides into the aqueous phase and away from the hydrophobic air phase may have occurred during gel formation, limiting the concentration of peptide at the gel surface. Alternatively, electrostatic interactions between cationic Lys side chains and the negatively charged titanium oxide surface<sup>55</sup> may compete with interactions between DOPA and the oxide surface. These and other possible explanations are currently under investigation.

Finally, we studied the effect of DOPA oxidation on adhesion strength to Ti. During curing of MAPs, DOPA is oxidized to semiquinone or quinone,<sup>56–58</sup> the latter being the reactive species that give rise to solidification of the adhesive plaque. In an earlier study by Deming and co-workers, DOPA–Lys copolypeptides were synthesized and studied as adhesives for bonding metal surfaces together.<sup>43</sup> Bond strengths were found to decrease in the presence of oxidizing agent, leading the authors to suggest that unoxidized DOPA is responsible for adhesion whereas oxidized DOPA leads to cross-linking and bulk solidification of the adhesive. Unfortunately, the macroscopic lap shear methodology previously used cannot unambiguously differentiate between cohesive and adhesive contributions to the measured shear strength values. One advantage of the JKR method used in the current study is that we can decouple the cohesive and adhesive contributions. Investigating the effects of DOPA oxidation was facilitated by addition of oxidizing agents to the medium, which significantly decreased  $W_{adh}$  (Figure 4) but did not change the bulk (cohesive) properties of the gel. Thus, our experimental model unequivocally demonstrates that work of adhesion of DOPA-containing hydrogels to a metal surface is decreased upon oxidation of the catechol, confirming the earlier conclusions of Deming and co-workers.<sup>43</sup> This method is versatile and can be easily extended to investigate more sophisticated peptide compositions and characterize adhesion to other surfaces such as tissues. Such studies may further elucidate the role of DOPA and other residues in mussel adhesion and lead to clinically useful synthetic hydrogels.

## Summary

Mussel adhesive protein mimetic block copolymers were synthesized and formulated into aqueous solutions capable of rapid photocuring into adhesive hydrogels. The block copolymer design facilitated rapid free-radical photopolymerization and high DOPA content compared to previously reported DOPA hydrogels. A contact mechanics method was used to probe the bulk physical properties of the hydrogels and work of adhesion for contact between the hydrogels and a Ti surface in aqueous buffer. The DOPA-containing hydrogels exhibited moduli of 30–40 kPa, similar to that of soft tissues. Work of adhesion increased with increasing DOPA content in the hydrogels, reaching a maximum value of 410 mJ/m<sup>2</sup> for polymers containing 10 wt % DOPA. Oxidation of the gel-bound DOPA significantly reduced work of adhesion to Ti, indicating DOPA in its reduced form is responsible for the strong water-resistant adhesion to Ti. The DOPA-functionalized block copolymers described here can potentially function as in situ gel forming bioadhesive materials suitable for tissue repair and regeneration.

## References and Notes

- (1) Sawhney, A. S.; Pathak, C. P.; Hubbell, J. A. *Macromolecules* **1993**, *26*, 581–7.
- (2) Lyman, M. D.; Melanson, D.; Sawhney, A. S. *Biomaterials* **1996**, *17*, 359–64.
- (3) Lovich, M. A.; Philbrook, M.; Sawyer, S.; Weselcouch, E.; Edelman, R. E. *Am. J. Physiol.* **1998**, *275*, H2236–H2242.
- (4) Burdick, J. A.; Philpott, L. M.; Anseth, K. S. *J. Polym. Sci., Part A: Polym. Chem.* **2001**, *39*, 683–692.
- (5) Ranger, W. R.; Halpin, D.; Sawhney, A. S.; Lyman, M.; Locicero, J. *Am. Surg.* **1997**, *63*, 788–95.
- (6) Alleyne, C. H., Jr.; Cawley, C. M.; Barrow, D. L.; Poff, B. C.; Powell, M. D.; Sawhney, A. S.; Dillehay, D. L. *J. Neurosurg.* **1998**, *88*, 308–13.
- (7) Waite, J. H. *Integr. Comp. Biol.* **2002**, *42*, 1172–1180.
- (8) Yu, M.; Deming, T. J. *Macromolecules* **1998**, *31*, 4739–45.
- (9) Yamamoto, H. *J. Adhes. Sci. Technol.* **1987**, *1*, 177–83.
- (10) Yamamoto, H.; Kuno, S.; Nagai, A.; Nishida, A.; Yamauchi, S.; Ikeda, K. *Int. J. Biol. Macromol.* **1990**, *12*, 305–10.
- (11) Tatehata, H.; Mochizuki, A.; Kawashima, T.; Yamashita, S.; Yamamoto, H. *J. Appl. Polym. Sci.* **2000**, *76*, 929–937.
- (12) Huang, K.; Lee, B. P.; Ingram, D.; Messersmith, P. B. *Biomacromolecules* **2002**, *3*, 397–406.
- (13) Lee, B. P.; Dalsin, J. L.; Messersmith, P. B. *Biomacromolecules* **2002**, *3*, 1038–47.
- (14) Dalsin, J. L.; Hu, B.-H.; Lee, B. P.; Messersmith, P. B. *J. Am. Chem. Soc.* **2003**, *125*, 4253–4258.
- (15) Hu, B.-H.; Messersmith, P. B. *J. Am. Chem. Soc.* **2003**, *125*, 14298–13299.
- (16) Lee, B. P.; Huang, K.; Nunalee, F. N.; Shull, K. R.; Messersmith, P. B. *J. Biomater. Sci., Polym. Ed.* **2004**, *15*, 449–464.
- (17) Dalsin, J. L.; Lin, L.; Tosatti, S.; Voeroes, J.; Textor, M.; Messersmith, P. B. *Langmuir* **2005**, *21*, 640–646.
- (18) Statz, A. R.; Meagher, R. J.; Barron, A. E.; Messersmith, P. B. *J. Am. Chem. Soc.* **2005**, *127*, 7972–7973.



- (19) Khudyakov, I. V.; Legg, J. C.; Purvis, M. B.; Overton, B. J. *Ind. Eng. Chem. Res.* **1999**, *38*, 3353–3359.
- (20) Dossot, M.; Sylla, M.; Allonas, X.; Merlin, A.; Jacques, P.; Fouassier, J.-P. *J. Appl. Polym. Sci.* **2000**, *78*, 2061–2074.
- (21) Fujisawa, S.; Ishihara, M.; Kadoma, Y. *SAR QSAR Environ. Res.* **2002**, *13*, 617–27.
- (22) Sichel, G.; Corsaro, C.; Scalia, M.; Sciuto, S.; Geremia, E. *Cell Biochem. Funct.* **1987**, *5*, 123–8.
- (23) Fuller, W. D.; Verlander, M. S.; Goodman, M. *Biopolymers* **1976**, *15*, 1869–1871.
- (24) Fuller, W. D.; Verlander, M. S.; Goodman, M. *Biopolymers* **1978**, *17*, 2939–43.
- (25) Flood, R. W.; Geller, T. P.; Petty, S. A.; Roberts, S. M.; Skidmore, J.; Volk, M. *Org. Lett.* **2001**, *3*, 683–686.
- (26) Floudas, G.; Papadopoulos, P.; Klok, H.-A.; Vandermeulen, G. W. M.; Rodriguez-Hernandez, J. *Macromolecules* **2003**, *36*, 3673–3683.
- (27) Hrkach, J. S.; Ou, J.; Lotan, N.; Langer, R. *Macromolecules* **1995**, *28*, 4736–9.
- (28) Klok, H.-A.; Hernandez, J. R.; Becker, S.; Mullen, K. *J. Polym. Sci., Part A: Polym. Chem.* **2001**, *39*, 1572–1583.
- (29) Rodriguez-Hernandez, J.; Gatti, M.; Klok, H.-A. *Biomacromolecules* **2003**, *4*, 249–58.
- (30) Nakonieczna, L.; Przycgodzen, W.; Chimiak, A. *Liebigs Ann. Chem.* **1994**, 1055.
- (31) Reed, N. N.; Janda, K. D. *J. Org. Chem.* **2000**, *65*, 5843–5845.
- (32) Johnson, K. L.; Kendall, K.; Roberts, A. D. *Proc. R. Soc. London* **1971**, *324*, 301–13.
- (33) Araujo, P. Z.; Morando, P. J.; Blesa, M. A. *Langmuir*, in press.
- (34) Martin, S.; Kesselman, J.; Park, D.; Lewis, N.; Hoffmann, M. *Environ. Sci. Technol.* **1996**, *30*, 2535–42.
- (35) Dalsin, J. L.; Lin, L.; Messersmith, P. B. *Polym. Mater. Sci. Eng.* **2004**, *90*, 247–248.
- (36) Hertz, H. *J. Reine Angew. Math.* **1881**, *92*, 156–171.
- (37) Shull, K. R.; Chen, W.-L. *Interface Sci.* **2000**, *8*, 95–110.
- (38) Flanagan, C. M.; Crosby, A. J.; Shull, K. R. *Macromolecules* **1999**, *32*, 7251–7262.
- (39) Waite, J. H. *Int. J. Adhes. Adhes.* **1987**, *7*, 9–14.
- (40) Yamamoto, H. *Biotechnol. Genet. Eng. Rev.* **1996**, *13*, 133–65.
- (41) Papov, V. V.; Diamond, T. V.; Biemann, K.; Waite, J. H. *J. Biol. Chem.* **1995**, *270*, 20183–92.
- (42) Waite, J. H.; Qin, X. *Biochemistry* **2001**, *40*, 2887–93.
- (43) Yu, M.; Hwang, J.; Deming, T. J. *J. Am. Chem. Soc.* **1999**, *121*, 5825–5826.
- (44) Andrzejewska, E.; Linden, L. A.; Rabek, J. F. *Macromol. Chem. Phys.* **1998**, *199*, 441–449.
- (45) Mowery, C. L.; Crosby, A. J.; Ahn, D.; Shull, K. R. *Langmuir* **1997**, *13*, 6101–6107.
- (46) Flanagan, C. M.; Shull, K. R. *Langmuir* **1999**, *15*, 4966–4974.
- (47) Deruelle, M.; Leger, L.; Tirrell, M. *Macromolecules* **1995**, *28*, 7419–28.
- (48) Dillow, A. K.; Ochsenhirt, S. E.; McCarthy, J. B.; Fields, G. B.; Tirrell, M. *Biomaterials* **2001**, *22*, 1493–505.
- (49) Stile, R. A.; Shull, K. R.; Healy, K. E. *Langmuir* **2003**, *19*, 1853–1860.
- (50) Sousa, S. R.; Moradas-Ferreira, P.; Saramago, B.; Melo, L. V.; Barbosa, M. A. *Langmuir* **2004**, *20*, 9745–54.
- (51) Janchen, G.; Mertig, M.; Pompe, W. *Surf. Interface Anal.* **1999**, *27*, 444–449.
- (52) Yamamoto, H.; Ogawa, T.; Ohkawa, K. *J. Colloid Interface Sci.* **1995**, *176*, 111–16.
- (53) Yamamoto, H.; Ohara, S.; Tanisho, H.; Ohkawa, K.; Nishida, A. *J. Colloid Interface Sci.* **1993**, *156*, 515–517.
- (54) Tatehata, H.; Mochizuki, A.; Ohkawa, K.; Yamada, M.; Yamamoto, H. *J. Adhes. Sci. Technol.* **2001**, *15*, 1003–13.
- (55) Kenausis, G. L.; Voros, J.; Elbert, D. L.; Huang, N.; Hofer, R.; Ruiz-Taylor, L.; Textor, M.; Hubbell, J. A.; Spencer, N. D. *J. Phys. Chem. B* **2000**, *104*, 3298–3309.
- (56) Rzepecki, L. M.; Nagafuchi, T.; Waite, J. H. *Arch. Biochem. Biophys.* **1991**, *285*, 17–26.
- (57) Sugumaran, M. *Adv. Insect Physiol.* **1998**, *27*, 230–334.
- (58) Waite, J. H. *Comp. Biochemistry Physiol., Part B: Comp. Biochem.* **1990**, *97*, 19–29.

MA0518959